Inorg. Chem. **2009**, *48*, 1062−1068

3-D Lanthanide Metal-Organic Frameworks: Structure, Photoluminescence, and Magnetism

Cory A. Black,[†] José Sánchez Costa,[†] Wen Tian Fu,[†] Chiara Massera,[§] Olivier Roubeau,[‡] Simon J. Teat,[||] Guillem Aromí,[⊥] Patrick Gamez,*[,†] and Jan Reedijk*[,†]

Leiden Institute of Chemistry, Leiden University, P.O. Box 9502, 2300 RA Leiden, The Netherlands, Université Bordeaux 1, CNRS-CRPP, 115 avenue du Dr. A. Schweitzer, 33600 Pessac, France, Università degli Studi di Parma, Viale G. Usberti 17/A, 43100 Parma, Italy, ALS, Berkeley Laboratory, 1 Cyclotron Road, MS2-400, Berkeley, California 94720, and Universitat de Barcelona, Departament de Química Inorgànica, Grup d'Interaccions Magnètiques, Diagonal 647, 08028, Barcelona, Spain

Received September 18, 2008

A series of isostructural three-dimensional metal-organic frameworks $[Pr_2(N\text{-}BDC)_3(dmf)_4]_\infty$ (**1**), $\{[Eu_2(N\text{-}BDC)_3(dmf)_4]\cdot 2DMF\}_\infty$ (**2**·2DMF), $[Gd_2(N\text{-}BDC)_3(dmf)_4]_\infty$ (**3**), $\{[Tb_2(N\text{-}BDC)_3(dmf)_4]\cdot 2DMF\}_\infty$ (**4**·2DMF), $\{[Dy_2(N\text{-}BDC)_3(dmf)_4]\cdot 2DMF\}_\infty$ (**5**·2DMF) (N-H_2BDC = 2-amino-1,4-benzenedicarboxylic acid; DMF = N,N′-dimethylformamide) with cubic $4^{12}\cdot 6^3$ topology have been synthesized using solvothermal conditions. The networks were generated via formation of a dinuclear Ln_2 secondary building block, involving the dicarboxylate ligand as a bridge. The luminescent properties of the Tb^{III} and Eu^{III} complexes were studied and showed characteristic emissions at room temperature. Antiferromagnetic interactions between Ln^{III} ions were observed from magnetic susceptibility data.

Introduction

The exponential growth[1] of the field of metal-organic materials, particularly metal-organic frameworks (MOFs), can be attributed to their fascinating network topologies coupled with their many potential applications. The applications envisaged for these well-ordered frameworks include gas storage[2,3] and separation,[4] catalysis,[5,6] enantioselective separation,[7,8] luminescent sensing,[9,10] and the preparation of new magnetic materials.[11,12] Even more remarkably, these applications can be combined and integrated into individual frameworks to form multifunctional MOFs.[9] MOFs can be readily prepared from the simple combination and self-assembly of metal ion nodes with organic bridging ligands containing divergent donor atoms. Such a facile synthesis has been an important factor in their remarkable popularity.

Lanthanide (Ln)-containing MOFs have attracted interest due to their ability to incorporate both photoluminescent centers and magnetic properties, making them ideal for developing new multifunctional materials.[13] Furthermore, the high affinity of lanthanides for oxygen donor atoms makes carboxylates excellent candidates as bridging ligands for

* To whom correspondence should be addressed. Tel: +31 71 5274260. Fax: +31 71 5274671. E-mail: p.gamez@chem.leidenuniv.nl (P.G.), reedijk@chem.leidenuniv.nl (J.R.).
[†] Leiden University.
[§] Università degli Studi di Parma.
[‡] Université Bordeaux 1.
[||] ALS, Berkeley Laboratory.
[⊥] Universitat de Barcelona.

(1) James, S. L. *Chem. Soc. Rev.* **2003**, *32*, 276–288.
(2) Kaye, S. S.; Dailly, A.; Yaghi, O. M.; Long, J. R. *J. Am. Chem. Soc.* **2007**, *129*, 14176–14177.
(3) Millward, A. R.; Yaghi, O. M. *J. Am. Chem. Soc.* **2005**, *127*, 17998–17999.
(4) Bastin, L.; Barcia, P. S.; Hurtado, E. J.; Silva, J. A. C.; Rodrigues, A. E.; Chen, B. *J. Phys. Chem. C* **2008**, *112*, 1575–1581.
(5) Sawaki, T.; Aoyama, Y. *J. Am. Chem. Soc.* **1999**, *121*, 4793–4798.
(6) Gandara, F.; Gornez-Lor, B.; Gutierrez-Puebla, E.; Iglesias, M.; Monge, M. A.; Proserpio, D. M.; Snejko, N. *Chem. Mater.* **2008**, *20*, 72–76.
(7) Wu, C. D.; Hu, A.; Zhang, L.; Lin, W. B. *J. Am. Chem. Soc.* **2005**, *127*, 8940–8941.
(8) Seo, J. S.; Whang, D.; Lee, H.; Jun, S. I.; Oh, J.; Jeon, Y. J.; Kim, K. *Nature* **2000**, *404*, 982–986.
(9) Harbuzaru, B. V.; Corma, A.; Rey, F.; Atienzar, P.; Jordá, J. L.; García, H.; Ananias, D.; Carlos, L. D.; Rocha, J. *Angew. Chem., Int. Ed.* **2008**, *47*, 1080–1083.
(10) Park, Y. K.; Choi, S. B.; Kim, H.; Kim, K.; Won, B. H.; Choi, K.; Choi, J. S.; Ahn, W. S.; Won, N.; Kim, S.; Jung, D. H.; Choi, S. H.; Kim, G. H.; Cha, S. S.; Jhon, Y. H.; Yang, J. K.; Kim, J. *Angew. Chem., Int. Ed.* **2007**, *46*, 8230–8233.
(11) Maspoch, D.; Ruiz-Molina, D.; Wurst, K.; Domingo, N.; Cavallini, M.; Biscarini, F.; Tejada, J.; Rovira, C.; Veciana, J. *Nat. Mater.* **2003**, *2*, 190–195.
(12) Ye, Q.; Fu, D. W.; Tian, H.; Xiong, R. G.; Chan, P. W. H.; Huang, S. P. D. *Inorg. Chem.* **2008**, *47*, 772–774.
(13) Guo, X. D.; Zhu, G. S.; Li, Z. Y.; Chen, Y.; Li, X. T.; Qiu, S. L. *Inorg. Chem.* **2006**, *45*, 4065–4070.

10.1021/ic8017826 CCC: $40.75
Published on Web 01/07/2009

Scheme 1

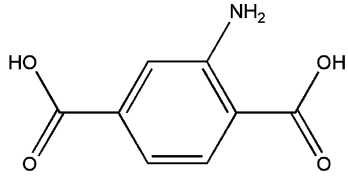

2-amino-1,4-benzene dicarboxylic acid - N-H_2BDC

preparing stable architectures.[14] The different emission and magnetic properties of Ln ions ensures that, through judicious choice, it is possible to precisely tailor individual MOFs depending on specific requirements.

An important objective in this field is that of reproducibility and predictability in network topology. This can be achieved in a number of ways, with one of the most successful being the inclusion of secondary building units (SBUs), conceptual units generated in situ upon which the structure is built around.[15−17] In MOF chemistry, SBU nodes are often formed from metal-oxide clusters which impart both stability to the network and fixed coordination geometries for expansion of the structure. The most dominant ligands used as links within SBUs in MOF literature have been rigid anionic carboxylates, particularly since the early work of Yaghi's MOF-5[18] and the subsequent syntheses of exceptionally high surface area MOFs.[19,20] Indeed, the salient virtues inherent to the choice of carboxylates as ligands, including SBU formation and structural reproducibility, have been highly lauded by Yaghi and Rowsell.[21]

We have employed the ligand 2-amino-1,4-benzene dicarboxylic acid (N-H_2BDC; Scheme 1), which provides divergent sites for polymer formation together with an amino group intended to occupy the cavities of the expected network. Recently, we described the first crystallographic evidence for the postsynthetic functional group modification of this amino functional group in $[Gd_2(N\text{-}BDC)_3(dmf)_4]_\infty$ (**3**).[22]

The versatility of the N-H_2BDC ligand is demonstrated by the structures described in the literature involving lanthanide building blocks analogous to those described in this work.[23−25] Zheng et al. describe Pr^{III}, Tb^{III}, Eu^{III},[23] and Dy^{III}[24] three-dimensional coordination polymers prepared using hydrothermal aqueous conditions. In a similar fashion to the structures reported herein, the amino groups do not coordinate to the metal ion and instead occupy the channels, where they are involved in hydrogen-bonding interactions with H_2O guest molecules. Although the Tb^{III}, Eu^{III}, and Dy^{III} compounds are isostructural, the Pr^{III} complex adopts a different topology, and in contrast to the other three structures, it exhibits two crystallographically distinct Pr^{III} ions.

Another Pr(N-BDC) structure, namely, $\{[Pr_3(N\text{-}BDC)_2(HN\text{-}BDC)_4]\cdot(NO_3)\cdot 8H_2O\}_n$, has been reported by Cheng et al.[25] The authors use a slow diffusion technique to form the crystalline MOF, which contains 12 N-BDC ligands which coordinate through an unusual pentadentate bridging mode to a trinuclear metal cluster. The resulting three-dimensional MOF is found to be stable to the loss of the guest water molecules. Interestingly, the network is able to adsorb four methanol molecules per Pr_3 cluster unit.

Herein, we describe the solvothermal synthesis and X-ray crystal structure characterization of five new, isostructural metal-organic frameworks using a series of lanthanides with 2-amino-1,4-benzene dicarboxylic acid (N-H_2BDC). By including lanthanides which have a strong preference for high coordination numbers, we have been able to reproducibly form a dinuclear SBU to create isotopological networks. Photoluminescence spectra were collected for the Eu and Tb complexes. Furthermore, magnetic susceptibility studies of these materials showed all compounds to display antiferromagnetic behavior.

Experimental Section

In a typical synthesis, a mixture of N-H_2BDC and $M(NO_3)_3\cdot nH_2O$ [M = Pr^{III} (**1**), Eu^{III} (**2**·2DMF), Gd^{III} (**3**), Tb^{III} (**4**·2DMF), Dy^{III} (**5**·2DMF); $n = 5$ (**2**·2DMF, **4**·2DMF) or 6 (**1**, **3**, **5**·2DMF)] in DMF (20 mL) was placed in an oven at 120 °C overnight, from which crystals were obtained.

Materials. All chemicals purchased were reagent grade and used without further purification. Elemental analyses (C, H, and N) were performed on a Perkin-Elmer 2400 series II analyzer. FT-IR spectra were recorded as neat samples in the range 400−4000 cm^{-1} on a Perkin-Elmer Paragon 1000 FTIR spectrophotometer, equipped with a Golden Gate ATR device, using the reflectance technique. Thermogravimetric analyses (TGA) were carried out with a Setaram TAG24 instrument. The emission spectra were recorded with a Perkin-Elmer LS50B luminescence spectrometer. Variable-temperature magnetic susceptibilities were measured on a Quantum Design MPMS-7 SQUID magnetometer. Diamagnetic corrections were made with Pascal's constants for all of the constituent atoms.

$[Pr_2(N\text{-}BDC)_3(dmf)_4]_\infty$ (1). $Pr(NO_3)_3\cdot 6H_2O$ (96 mg, 0.22 mmol) dissolved in DMF (10 mL) was added to a solution of N-H_2BDC (60 mg, 0.33 mmol) in DMF (10 mL) in a glass tube (Duran culture tube, diameter 18 mm, height 180 mm). The tube was sealed; the contents were well mixed and then placed in an oven at 120 °C for 20 h, resulting in the formation of single crystals in high yield (101 mg, 82%). The crystals were filtered, washed with a little DMF (∼5 mL), and then dried in the vacuum oven for 15 min. Anal.

(14) Wu, J. Y.; Yeh, T. T.; Wen, Y. S.; Twu, J.; Lu, K. L. *Cryst. Growth Des.* **2006**, *6*, 467–473.
(15) Eddaoudi, M.; Kim, J.; Rosi, N.; Vodak, D.; Wachter, J.; O'Keeffe, M.; Yaghi, O. M. *Science* **2002**, *295*, 469–472.
(16) Eddaoudi, M.; Moler, D. B.; Li, H. L.; Chen, B. L.; Reineke, T. M.; O'Keeffe, M.; Yaghi, O. M. *Acc. Chem. Res.* **2001**, *34*, 319–330.
(17) O'Keeffe, M.; Eddaoudi, M.; Li, H. L.; Reineke, T.; Yaghi, O. M. *J. Solid State Chem.* **2000**, *152*, 3–20.
(18) Li, H.; Eddaoudi, M.; O'Keeffe, M.; Yaghi, O. M. *Nature* **1999**, *402*, 276–279.
(19) Chae, H. K.; Siberio-Perez, D. Y.; Kim, J.; Go, Y.; Eddaoudi, M.; Matzger, A. J.; O'Keeffe, M.; Yaghi, O. M. *Nature* **2004**, *427*, 523–527.
(20) Ferey, G.; Mellot-Draznieks, C.; Serre, C.; Millange, F.; Dutour, J.; Surble, S.; Margiolaki, I. *Science* **2005**, *309*, 2040–2042.
(21) Rowsell, J. L. C.; Yaghi, O. M. *Microporous Mesoporous Mater.* **2004**, *73*, 3–14.
(22) Costa, J. S.; Gamez, P.; Black, C. A.; Roubeau, O.; Teat, S. J.; Reedijk, J. *Eur. J. Inorg. Chem.* **2008**, 1551–1554.
(23) Xu, H. T.; Zheng, N. W.; Jin, X. L.; Yang, R. Y.; Wu, Y. G.; Ye, E. Y.; Li, Z. Q. *J. Mol. Struct.* **2003**, *655*, 339–342.
(24) Xu, H. T.; Zheng, N. W.; Jin, X. L.; Yang, R. Y.; Li, Z. Q. *J. Mol. Struct.* **2003**, *646*, 197–199.
(25) Chen, X. Y.; Zhao, B.; Shi, W.; Xia, J.; Cheng, P.; Liao, D. Z.; Yan, S. P.; Jiang, Z. H. *Chem. Mater.* **2005**, *17*, 2866–2874.

found for $[Pr_2(N\text{-}BDC)_3(dmf)_4]_\infty$: C, 38.58; H, 4.76; N, 9.10%. Calcd: C, 38.90; H, 3.90; N, 8.82%. Selected IR data (Neat): 3451 (w) ν(OH), 3345 (w) ν(NH), 2932 (w) υ(CH), 1665 (m) ν(CO), 1645 (m) ν_{as}(COO), 1539 (m) ν(C═C), 1496 (m) ν_s(COO), 1416 (m) ν(CO), 1373 (s) ν(CN), 1251 (m) ν(CO), 769 (s) δ(OCO), 672 (s) δ(═CH) cm^{-1}. The crystals were analyzed by single-crystal X-ray diffraction and by X-ray powder diffraction (see the Supporting Information).

$\{[Eu_2(N\text{-}BDC)_3(dmf)_4]\cdot 2DMF\}_\infty$ (2·2DMF). $Eu(NO_3)_3\cdot 5H_2O$ (99 mg, 0.23 mmol) dissolved in DMF (10 mL) was added to a solution of N-H_2BDC (62 mg, 0.34 mmol) in DMF (10 mL) in a glass tube (Duran culture tube, diameter 18 mm, height 180 mm). The tube was sealed; the contents were well mixed and then placed in an oven at 120 °C for 20 h, resulting in the formation of single crystals in good yield (106 mg, 73%). The crystals were filtered, washed with a little DMF (~5 mL), and then dried in the vacuum oven for 15 min. It has to be mentioned here that the MOFs most likely lose DMF solvent molecules during the drying and pick up atmospheric water upon air exposure. Anal. found for $\{[Eu_2(N\text{-}BDC)_3(dmf)_3]\cdot 2H_2O\}_\infty$ C, 36.21; H, 3.76; N, 7.57%. Calcd: C, 36.14; H, 3.68; N, 7.66%. Selected IR data (Neat): 3442 (w) ν(OH), 3345 (w) ν(NH), 2932 (w) ν(CH), 1665 (m) ν(CO), 1645 (m) ν_{as}(COO), 1539 (m) ν(C═C), 1496 (m) υ_s(COO), 1416 (m) ν(CO), 1373 (s) ν(CN), 1251 (m) ν(CO), 769 (s) δ(OCO), 672 (s) δ(═CH) cm^{-1}. The crystals were analyzed by single-crystal X-ray diffraction and by X-ray powder diffraction.

$[Gd_2(N\text{-}BDC)_3(dmf)_4]_\infty$ (3).[22] $Gd(NO_3)_3\cdot 6H_2O$ (300 mg, 0.67 mmol) dissolved in DMF (10 mL) was added to a solution of N-H_2BDC (181 mg, 1.00 mmol) in DMF (10 mL) in a glass tube (Duran culture tube, diameter 18 mm, height 180 mm). The tube was sealed; the contents were well mixed and then placed in an oven at 120 °C for 20 h, resulting in the formation of single-crystals in high yield (303 mg, 80%). The crystals were filtered, washed with a little DMF (~5 mL), and then dried in the vacuum oven for 15 min. Anal. found for $[Gd_2(N\text{-}BDC)_3(dmf)_4]_\infty$: C, 37.58; H, 3.67; N, 8.45%. Calcd: C, 37.79; H, 3.79; N, 8.57%. Selected IR data (Neat): 3445 (w) ν(OH), 3344 (w) ν(NH), 2931 (w) ν(CH), 1668 (m) ν(CO), 1649 (m) ν_{as}(COO), 1540 (m) ν(C═C), 1496 (m) υ_s(COO), 1417 (m) ν(CO), 1373 (s) ν(CN), 1252 (m) ν(CO), 770 (s) δ(OCO), 676 (s) δ(═CH) cm^{-1}. The crystals were analyzed by single-crystal X-ray diffraction and by X-ray powder diffraction.

$\{[Tb_2(N\text{-}BDC)_3(dmf)_4]\cdot 2DMF\}_\infty$ (4·2DMF)). $Tb(NO_3)_3\cdot 5H_2O$ (100 mg, 0.23 mmol) dissolved in DMF (10 mL) was added to a solution of N-H_2BDC (61 mg, 0.34 mmol) in DMF (10 mL) in a glass tube (Duran culture tube, diameter 18 mm, height 180 mm). The tube was sealed; the contents were well mixed and then placed in an oven at 120 °C for 20 h, resulting in the formation of single crystals in high yield (106 mg, 82%). The crystals were filtered, washed with a little DMF (~5 mL), and then dried in the vacuum oven for 15 min. Anal. found: for $[Tb_2(N\text{-}BDC)_3(dmf)_4]_\infty$: C, 37.42; H, 4.28; N, 8.99%. Calcd: C, 37.68; H, 3.78; N, 8.54%. Selected IR data (Neat): 3453 (w) ν(OH), 3343 (w) ν(NH), 2936 (w) ν(CH), 1669 (m) ν(CO), 1651 (m) ν_{as}(COO), 1544 (m) ν(C═C), 1497 (m) ν_s(COO), 1419 (m) ν(CO), 1374 (s) ν(CN), 1253 (m) ν(CO), 770 (s) δ(OCO), 676 (s) δ(═CH) cm^{-1}. The crystals were analyzed by single-crystal X-ray diffraction and by X-ray powder diffraction.

$\{[Dy_2(N\text{-}BDC)_3(dmf)_4]\cdot 2DMF\}_\infty$ (5·2DMF). $Dy(NO_3)_3\cdot 6H_2O$ (91 mg, 0.20 mmol) dissolved in DMF (10 mL) was added to a solution of N-H_2BDC (60 mg, 33 mmol) in DMF (10 mL) in a glass tube (Duran culture tube, diameter 18 mm, height 180 mm). The tube was sealed; the contents were well mixed and then placed in an oven at 120 °C for 20 h, resulting in the formation of single crystals in good yield (75 mg, 66%). The crystals were filtered, washed with a little DMF (~5 mL), and then dried in the vacuum oven for 15 min. After drying, it appears that the material takes up atmospheric water molecules (see the Infrared Spectra section below). Anal. found for $[Dy_2(N\text{-}BDC)_3(dmf)_4]_\infty\cdot H_2O$: C, 36.43; H, 4.39; N, 8.75%. Calcd: C, 36.87; H, 3.87; N, 8.36%. The deviations for %H and %N might be due to traces of remaining DMF. Selected IR data (Neat): 3471 (w) ν(OH), 3349 (w) ν(NH), 2936 (w) ν(CH), 1666 (m) ν(CO), 1654 (m) ν_{as}(COO), 1541 (m) ν(C═C), 1497 (m) ν_s(COO), 1419 (m) ν(CO), 1373 (s) ν(CN), 1253 (m) ν(CO), 771 (s) δ(OCO), 677 (s) δ(═CH) cm^{-1}. The crystals were analyzed by single-crystal X-ray diffraction and by X-ray powder diffraction.

Structural Determination. Measurements on single crystals of **1** were performed with a Nonius Kappa CCD diffractometer with graphite-monochromated Mo Kα radiation (λ = 0.71073 Å). DENZO-SMN was used for data integration and SCALEPACK corrected data for Lorentz-polarization effects.[26] The absorption correction was performed with MULABS as implemented in PLATON.[27] The structure was solved by direct methods with SIR92,[28] and the refinement and all further calculations were carried out using the SHELX-TL suite.[29] All non-hydrogen atoms were refined anisotropically. Geometrical restraints were used in modeling the disordered amine groups. Displacement parameter restraints were used in modeling the ligands and solvent molecules. Hydrogen atoms were placed geometrically on their riding atom where possible. Residual electron density peaks in voids of the structure could not be modeled satisfactorily. These were taken into account by the SQUEEZE function of PLATON, which resulted in a significant improvement of the quality of the structure. The recovered electron density of 14.5 in voids as large as 300 $Å^3$ likely corresponds to diffuse disordered partial solvent (DMF) molecules.

X-ray crystallographic data for a colorless crystal of compound **2**·2DMF were collected on station 11.3.1 of the Advanced Light Source at Lawrence Berkeley National Laboratory, at 0.7749 Å, from a silicon 111 monochromator using a Bruker APEX II CCD diffractometer. The data were corrected for absorption effects with SADABS.[30] The structure was solved by direct methods with SIR97,[31] and the refinement and all further calculations were carried out using the SHELX-TL suite.[29] All non-hydrogen atoms with the exception of the disordered DMF solvent molecules were refined anisotropically. Geometrical restraints were used in modeling the disordered amine groups. Displacement parameter restraints were used in modeling the ligands, as well as bound and free solvent molecules. Hydrogen atoms were placed geometrically on their riding atom where possible.

The structure of compound **3** has been reported previously (CCDC 666828).[22]

Measurements on single crystals of **4**·2DMF and **5**·2DMF were carried out at 173 K on a Bruker AXS Smart 1000 single-crystal diffractometer (Mo Kα radiation) equipped with a CCD area detector. The data reductions were performed using the SAINT[32] and SADABS[33] programs. The structures were solved by direct

(26) Otwinowski, Z.; Minor, W. *Macromol. Crystallogr. A* **1997**, *276*, 307–326.
(27) Spek, A. L. *J. Appl. Crystallogr.* **2003**, *36*, 7–13.
(28) Altomare, A.; Cascarano, G.; Giacovazzo, C.; Guagliardi, A.; Burla, M. C.; Polidori, G.; Camalli, M. *J. Appl. Crystallogr.* **1994**, *27*, 435.
(29) *SHELX-TL*; Bruker AXS: Madison, WI, 2001.
(30) *SADABS*; Bruker AXS: Madison, WI, 2004.
(31) Altomare, A.; Burla, M. C.; Camalli, M.; Cascarano, G. L.; Giacovazzo, C.; Guagliardi, A.; Moliterni, A. G. G.; Polidori, G.; Spagna, R. *J. Appl. Crystallogr.* **1999**, *32*, 115–119.
(32) *SAINT, Software Users Guide*; Analytical X-ray Systems: Madison, WI, 1999.
(33) Sheldrick, G. M. *SADABS*, v2.03; University of Göttingen: Göttingen, Germany, 1999.

Table 1. Crystal Data and Structure Refinement Information for Compounds **1**−**5**

compound	**1**	**2**·2DMF	**3**	**4**·2DMF	**5**·2DMF
formula	$C_{36}H_{43}Pr_2N_7O_{16}$	$C_{42}H_{57}Eu_2N_9O_{18}$	$C_{36}H_{43}Gd_2N_7O_{16}$	$C_{42}H_{57}Tb_2N_9O_{18}$	$C_{42}H_{57}Dy_2N_9O_{18}$
fw	1111.59	1279.88	1144.26	1293.81	1300.97
cryst syst	triclinic	triclinic	triclinic	triclinic	triclinic
space group	$P\bar{1}$	$P\bar{1}$	$P\bar{1}$	$P\bar{1}$	$P\bar{1}$
a/Å	10.4951(3)	10.4692(6)	10.4883(11)	10.5390(9)	10.5059(9)
b/Å	11.3396(3)	11.2307(7)	11.2214(12)	11.2180(9)	11.1476(9)
c/Å	12.7954(4)	12.7358(8)	12.7410(13)	12.8420(11)	12.7931(10)
α/deg	100.730(2)	101.237(2)	100.986(2)	101.472(1)	100.955(1)
β/deg	110.1420(10)	110.087(2)	110.352(2)	110.500(1)	110.450(1)
γ/deg	99.732(2)	99.626(2)	99.772(2)	99.257(1)	99.939(1)
V/Å^3	1359.05(7)	1334.08(14)	1334.0(2)	1349.0(2)	1330.93(19)
Z	1	1	1	1	1
T/K	293(2)	150(2)	150(2)	173(2)	173(2)
ρ/g cm^{-3}	1.358	1.502	1.421	1.593	1.623
μ/mm^{-1}	1.832	2.991	4.653	2.674	2.861
F(000)	554	602	561	646	648
data/params	6134/290	7327/379	4795/290	6447/271	71037/299
goodness-of-fit on F^{2a}	1.093	1.059	1.089	1.005	1.005
R_1 indices $[F_o > 4\sigma(F_o)]^b$	0.0484	0.0506	0.0401	0.0325	0.0431
wR_2 (all data)^b	0.1408	0.1548	0.1180	0.0945	0.1108
largest diff. peak and hole/eÅ^{-3}	1.223−1.503	1.560−1.001	1.575−1.777	2.361−1.466	3.384−2.091

^{a} Goodness-of-fit $S = [\sum w(F_o^2 - F_c^2)^2/(n-p)]^{1/2}$, where n is the number of reflections and p the number of parameters. ^{b} $R_1 = ||F_o| - |F_c||/\sum|F_o|$, $wR_2 = [\sum[w(F_o^2 - F_c^2)^2]/\sum[w(F_o^2)^2]]^{1/2}$.

methods using the SIR97 program[31] and refined on F_o^2 by full-matrix least-squares procedures, using the SHELXL-97 program.[34] The PLATON SQUEEZE procedure[35] was used to treat regions of diffuse solvent which could not be sensibly modeled in terms of atomic sites. Their contribution to the diffraction pattern was removed and the modified F_o^2 written to a new HKL file. The number of electrons thus located, 81 per unit cell, are included in the formula, formula weight, calculated density, μ, and F(000). This residual electron density was assigned to two molecules of DMF solvent per unit cell (two molecules of DMF would give 80 e$^-$).

The non-hydrogen atoms were refined with anisotropic atomic displacements with the exception of one coordinating DMF molecule and one disordered nitrogen atom of the amino group (presenting an occupancy factor of 0.25) in compound **4**·2DMF. The hydrogen atoms were included in the refinement at idealized geometries (C−H 0.95 Å) and refined "riding" on the corresponding parent atoms.

Crystallographic and experimental details for the different structures are summarized in Table 1. All details can be found in the Supporting Information for this paper in CIF format with CCDC numbers 702353 (**1**), 702354 (**2**·2DMF), 702355 (**4**·2DMF), and 702356 (**5**·2DMF). These data can be obtained free of charge from The Cambridge Crystallographic Data Centre via www.ccdc.cam.ac.uk/data_request/cif.

X-ray powder diffraction (XRPD) data for **1**−**5** were obtained using a Phillips Xpert Pro equipped with an X'celerator, with Cu Kα radiation ($\lambda \approx 1.5408$ Å), in the 2θ range 10−45°. The diffraction patterns were recorded at room temperature (see Figures S1−S5, Supporting Information).

Results and Discussion

Synthesis. All five complexes were formed using solvothermal synthesis by combining a N,N′-dimethylformamide (DMF) solution of $M(NO_3)_3 \cdot nH_2O$ [M = Pr^{III} (**1**), Eu^{III} (**2**·2DMF), Gd^{III} (**3**), Tb^{III} (**4**), Dy^{III} (**5**); n = 5 (**2**·2DMF, **4**), 6 (**1**, **3**, **5**)] with 2-amino-1,4-benzene dicarboxylic acid (N-H_2BDC) in DMF at 120 °C.

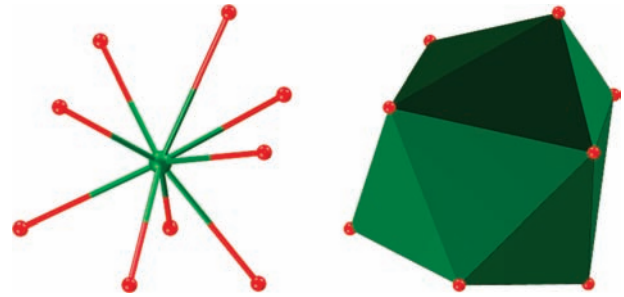

Figure 1. Left: View of the coordination environment around the Ln^{III} ions. Right: View of the 14-sided tetradecagon.

Structural Description. The five complexes formed as isostructural three-dimensional networks as determined by single-crystal X-ray crystallography. The asymmetric unit contained one and one-half N-BDC ligands, one Ln^{III} ion, and two coordinated DMF molecules. The Eu^{III}, Tb^{III}, and Dy^{III} structures, **2**·2DMF, **4**·2DMF, and **5**·2DMF, respectively, present another noncoordinated DMF solvent molecule. Figures S1−S5 (Supporting Information) illustrate the comparison between the experimental X-ray powder diffraction patterns of powdered samples of the compounds obtained in greater amounts and the theoretical patterns calculated from the corresponding single-crystal X-ray data. The experimental and theoretical patterns are almost identical, thus indicating that the preparation of these MOFs can be successfully achieved on a large scale. Each metal ion is coordinated to a total of nine oxygen atoms from two chelating and three bridging N-BDC ligands as well as from the two coordinated DMF molecules (Figure 1, left). The Ln^{III} ions have a tricapped trigonal-pyramidal geometry represented by a 14-sided tetradecagon (Figure 1, right). A dinuclear edge-sharing Ln^{III} cluster is thus generated by four bridging carboxylato groups from four ligands exhibiting two bridging modes (μ-O,O′-carboxylato and μ-O,O,O′-carboxylato, Figure 2). The distances between the metal ions within

(34) Sheldrick, G. M. *SHELXL-97-2*; University of Göttingen: Göttingen, Germany, 1997.
(35) van der Sluis, P.; Spek, A. L. *Acta Crystallogr., Sect. A* **1990**, *46*, 194–201.

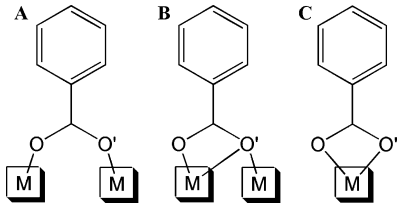

Figure 2. Different coordination modes observed for the N-BDC ligands. A: μ-O,O′-carboxylato. B: μ-O,O′,O′-carboxylato. C: O,O′-carboxylato.

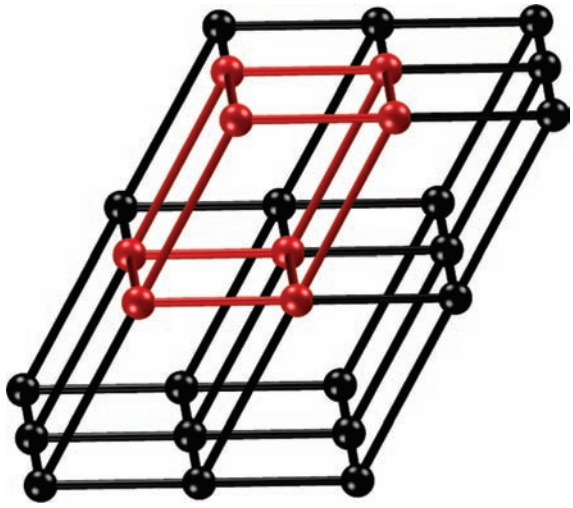

Figure 3. Stylized view of the $4^{12}\cdot6^3$ network topology of **1**−**5**. The repeating unit is shown in red.

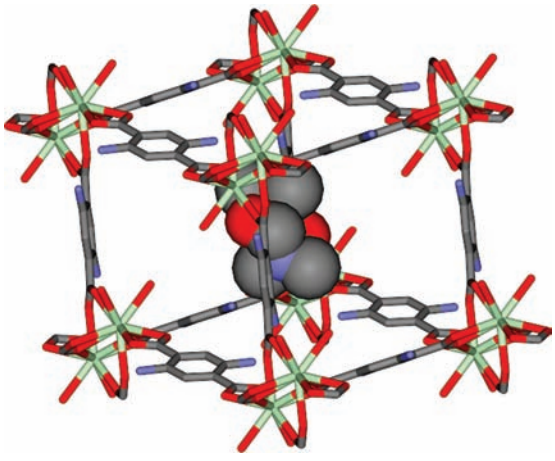

Figure 4. View of the repeating cubic unit for **1**−**5**. The guest DMF molecules which occupy the cavities are shown as space-filling atoms. Hydrogen atoms are omitted for clarity. The nitrogen atoms of the N-BDC ligands have occupancy factors of 0.5. Atom colors: green, Ln; red, O; blue, N; grey, C.

the cluster are 4.11954(8) (**1**), 4.0676(1) (**2**·2DMF), 4.07319(6) (**3**), 4.0892(1) (**4**·2DMF), and 4.0867(1) (**5**·2DMF) Å. The framework emerges through the connection of the metal clusters by virtue of the bifunctional nature of the N-BDC ligands (Figure 3). The dinuclear cluster acts therefore as a SBU,[16] which can be represented by a single octahedral node connected in three dimensions to describe a cubic network with a $4^{12}\cdot6^3$ topology (Figure 3). The coordinated DMF molecules are situated inside the cavities of the MOFs, thus occupying a large volume of free space (Figure 4). The noncoordinated DMF molecule in **2**·2DMF was involved in a $\pi-\pi$ stacking interaction with the ring containing C(4) [C(19)···ring centroid distance, 3.42(4) Å; C(19)···C(4) distance, 3.60(3) Å] as well as hydrogen-bonding interactions with adjacent coordinated DMF molecules [O(9)′···C distances in the range 3.14(3)−3.17(3) Å (van der Waals radii: 3.22 Å);[36] O(9)···H(13A) 2.64(3) Å] (Figure S6, Supporting Information).

With some exceptions, the amino groups in **1**−**5** occupy two crystallographic positions with site occupancy factors of 0.5. For **2**·2DMF, N1 and N1′ show occupancy factors of 0.2 and 0.3, respectively. Similarly, N1C in both **4**·2DMF and **5**·2DMF have occupancy factors of 0.25.

Infrared Spectra. The IR spectra for **1**−**5** (Figures S7−11, Supporting Information) are very similar and show characteristic bands for the asymmetric and symmetric stretch vibrations of the dicarboxylate groups at ∼1649 and ∼1496 cm^{-1}, respectively. The absence of bands at 3560−3500, 2700−2500 [ν(OH)], and 1700−1690 [ν(COOH)] confirmed the complete deprotonation of the N-BDC ligand.[37] A strong band at ∼1373 was attributed to the amino C−N stretch, and two N−H stretching bands were found at ∼3447 and ∼3345 cm^{-1}.[37] Finally, the C═O stretching frequency corresponding to DMF is observed at about 1668−1665 cm^{-1}. Taking into account that this characteristic band is detected around 1675 cm^{-1} for free DMF, these values suggest that the DMF molecules are coordinated to the metal nodes of the MOFs. Therefore, the DMF molecules sitting in the cavities (compounds **2**·2DMF, **4**·2DMF, and **5**·2DMF) are most likely lost during air exposure and are apparently replaced by water molecules. Indeed, for all spectra, a small absorption peak is noticed around 3470−3442 cm^{-1}, which can be ascribed to the symmetric stretching vibration of water molecules.

Thermogravimetric Analysis. TGA have been carried out for all compounds which show similar behaviors (Figures S12−S16, Supporting Information). From room temperature to about 100 °C, all five materials lose approximately 8% of their initial weight. This weight loss may be due to the loss of DMF molecules. Actually, the removal of two DMF molecules from **2**·2DMF, **4**·2DMF, and **5**·2DMF corresponds to a calculated weight loss of 12.1, 11.3, and 11.2%, respectively. It has to be mentioned that these coordination materials have probably exchanged part of their guest DMF molecules with atmospheric water upon air exposure prior to TG measurements. As a result, the 8% weight loss most likely represents the departure of DMF or water molecules. All five MOFs start to decompose at about 150 °C.

Luminescent Properties. The solid-state luminescent properties of **2**·2DMF and **4**·2DMF were investigated. When excited by ultraviolet light, the Eu^{III} coordination compound **2**·2DMF emitted red light. The emission spectrum was measured in the 550−740 nm range (λ_{ex} = 254 nm) and showed four major peaks assigned to the $^5D_0 \rightarrow {}^7F_J$ (J = 1−4) transitions, namely, $^5D_0 \rightarrow {}^7F_1$ (593 nm), $^5D_0 \rightarrow {}^7F_2$ (617 nm), $^5D_0 \rightarrow {}^7F_3$ (651 nm), and $^5D_0 \rightarrow {}^7F_4$ (698 nm) (Figure 5). The apparent absence of $^5D_0 \rightarrow {}^7F_0$ transition

(36) Bondi, A. *J. Phys. Chem.* **1964**, *68*, 441–451.
(37) Bellamy, L. J. *The Infrared Spectra of Complex Molecules*; John Wiley & Sons: New York, 1975.

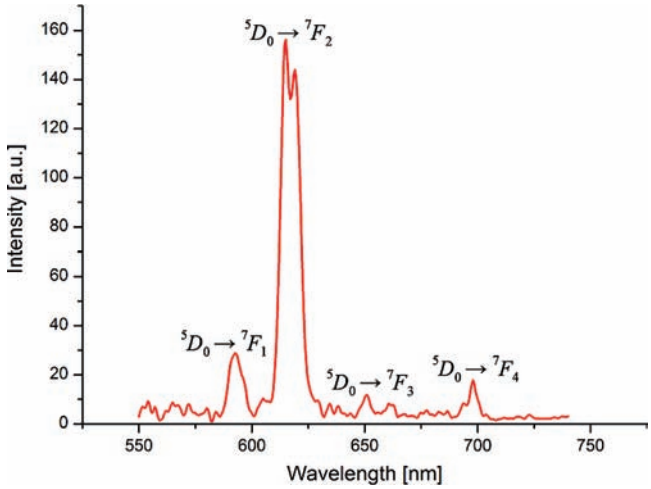

Figure 5. Solid-State Emission Spectrum of **2**·2DMF.

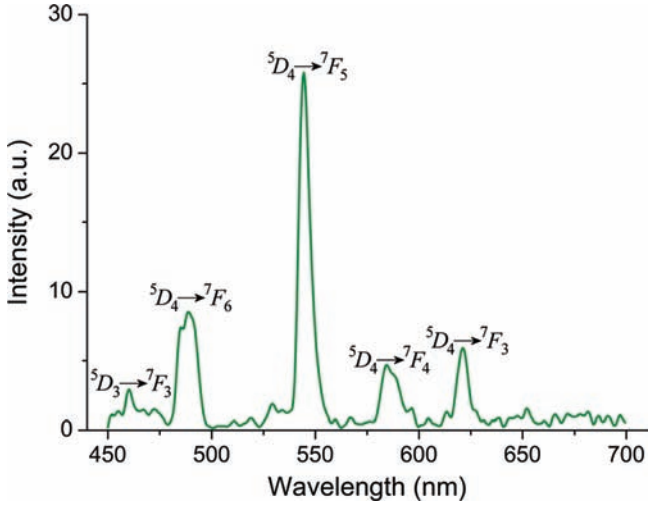

Figure 6. Solid-State Emission Spectrum of **4**·2DMF.

may be explained by the fact that this peak is usually clearly observed when the material belongs to the symmetry point group of C_{nv}, C_n, or C_s.[38] The spectrum is dominated by the intense $^5D_0 \rightarrow {}^7F_2$ electric dipole transition, which is split into two peaks at 615 and 619 nm. The intensity ratio $^5D_0 \rightarrow {}^7F_2/{}^5D_0 \rightarrow {}^7F_1$ was 5.4, much higher than 0.67, a typical value for a centrosymmetric Eu^{III} center.[39] This high ratio therefore signifies that the Eu^{III} ion adopted a noncentrosymmetric coordination environment, with no center of inversion, as observed on the single-crystal structure.[40]

The Tb^{III} complex **4**·2DMF emitted green light when excited by ultraviolet light (λ_{ex} = 365 nm). The emission spectrum of **4**·2DMF was collected in the range 450−700 nm and showed four peaks characteristic of Tb^{III} (Figure 6).[41] These peaks were assigned to the $^5D_4 \rightarrow {}^7F_J$ (J = 3−6) transitions, namely, $^5D_4 \rightarrow {}^7F_6$ (489 nm), $^5D_4 \rightarrow {}^7F_5$ (545 nm), $^5D_4 \rightarrow {}^7F_4$ (585 nm), and $^5D_4 \rightarrow {}^7F_3$ (621 nm). Besides the $^5D_4 \rightarrow {}^7F_J$ transitions, a weak emission line at ∼460 nm was observed, characteristic of the $^5D_3 \rightarrow {}^7F_3$ transition.

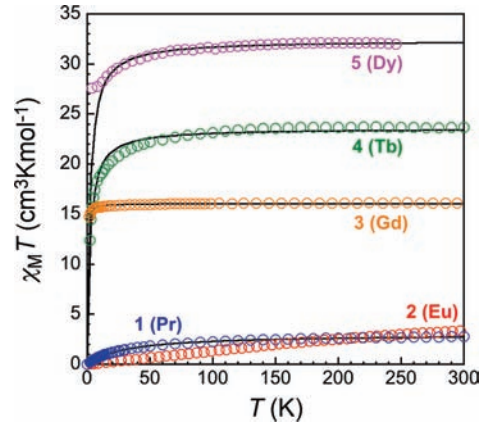

Figure 7. $\chi_M T$ vs T plot for compounds **1**−**5**. The data are shown per Ln_2, and only half of the data points are shown for clarity. The full lines represent the best-fit to a Curie−Weiss law (see text).

Magnetic Properties. Figure 7 shows the temperature dependences of χT (χ being the molar magnetic susceptibility expressed per mole of Ln_2 unit) for the five compounds under study. The Pr (**1**), Tb (**4**), and Dy (**5**) compounds presented a similar behavior with a χT value that remained stable from 300 K down to 80−100 K (at ca. 2.6, 23.7, and 32.2 cm^3 K mol^{-1} respectively), below which a decrease started to set in. For these three compounds, the lowering can be ascribed to the effects of the strong spin−orbit coupling of the lanthanide ions together with some weak antiferromagnetic interactions among them through carboxylato bridges. In the case of the Gd compound **3**, the χT remains stable at ca. 16.1 cm^3 K mol^{-1} down to lower temperatures, with a small decrease observed only below 20 K, which in this case can only be ascribed to weak antiferromagnetic interactions. Given the analogous molecular structures of compounds **1**−**5** and the observed very weak antiferromagnetic coupling for the Gd compound, one can expect similar exchange-coupling interactions for the other lanthanide compounds. This means that their magnetic properties are mostly dominated by the depopulation of excited states. Satisfactory fits of the experimental data for the other four compounds (above 10 K for the Dy compound) to a Curie−Weiss law ($\chi = C/(T - \theta)$) yield the following Curie (C) and Weiss (θ) constants: 3.01 cm^3 K mol^{-1} and −31.27 K for **1**, 16.07 cm^3 K mol^{-1} and −0.18 K for **3**, 23.57 cm^3 K mol^{-1} and −2.18 K for **4**, 32.39 cm^3 K mol^{-1} and −2.25 K for **5**. The Curie constants are reasonable for respectively two uncoupled Pr^{III} (S = 1°; $^3H_{4°}$; C = 2.9 cm^3 K mol^{-1}), Gd^{III} (S = 7/2°; $^8S_{0°}$; C = 15.75 cm^3 K mol^{-1}), Tb^{III} (S = 3°; $^7F_6$; C = 23.5 cm^3 K mol^{-1}), and Dy^{III} (S = 5/2°; $^6H_{15/2°}$; C = 28.34 cm^3 K mol^{-1}) ions. The negative Weiss constants suggest the presence of antiferromagnetic interactions among spin carriers, although, except for the Gd compound, magnetic anisotropy as well as depopulation of excited states (Starck sublevels of respectively the $^6H_{15/2}$, $^7F_6$, and $^3H_4$ states) probably also participate in θ.

For the Eu compound, the observed χT at room temperature is 3.34 cm^3 K mol^{-1}, slightly less than the value of 3

(38) Binnemans, K.; VanHerck, K.; Gorller Walrand, C. *Chem. Phys. Lett.* **1997**, *266*, 297–302.
(39) Klink, S. I.; Grave, L.; Reinhoudt, D. N.; van Veggel, F. C. J. M.; Werts, M. H. V.; Geurts, F. A. J.; Hofstraat, J. W. *J. Phys. Chem. A* **2000**, *104*, 5457–5468.
(40) Xia, J.; Zhao, B.; Wang, H. S.; Shi, W.; Ma, Y.; Song, H. B.; Cheng, P.; Liao, D. Z.; Yan, S. P. *Inorg. Chem.* **2007**, *46*, 3450–3458.
(41) Zhao, B.; Chen, X. Y.; Cheng, P.; Liao, D. Z.; Yan, S. P.; Jiang, Z. H. *J. Am. Chem. Soc.* **2004**, *126*, 15394–15395.

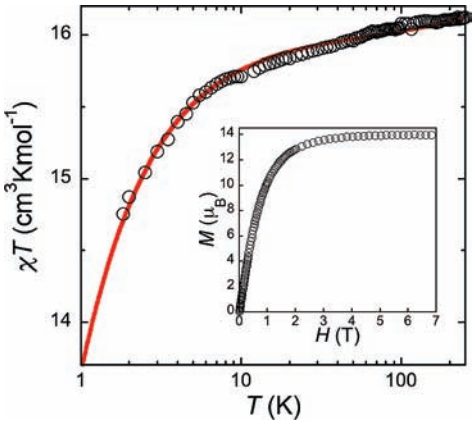

Figure 8. Semilog χT vs T plot for compound **3** at an applied field of 0.1 T (1000 Oe). The full line represents the best-fit to a simple exchange-coupled dinuclear Gd(III) model (see text). The inset shows an M vs H plot measured at 1.83 K.

calculated for two uncoupled Eu^{III} ions, allowing for population of the excited states with higher values of J at 293 K.[42] As the temperature is lowered, χT decreases continuously, which should be attributed to the depopulation of the Stark levels for the single Eu^{III} ions. At the lowest temperature, χT is close to zero, indicating a $J = 0$ ground state of the Eu^{III} ion ($^6F_0$). It is likely that some weak antiferromagnetic interactions are present as in the other four compounds, but hidden by the behavior of the single Eu^{III} ions.

For the four compounds of lanthanide ions with strong spin−orbit coupling, **1**, **2**, **4**, and **5**, a detailed analysis and model taking these anisotropic effects into account is beyond the scope of this study. On the other hand, the absence of anisotropic effects in the case of Gd^{III} allowed for a quantitative analysis of the magnetic exchange coupling in **3**. The magnetic properties are thus shown in more detail in Figure 8, in the form of χT versus T and M versus H plots (M is the molar magnetization calculated per formula unit, in Bohr magnetons), respectively at a 1000 Oe applied field and $T = 1.83$ K. χT remains almost constant down to ca. 30 K, with a very gradual small decrease from 16.12 cm^3 K mol^{-1} at 300 K down to 15.90 cm^3 K mol^{-1} at 30 K, probably due to temperature independent magnetism (TIP), and then decreases more and more rapidly as T is lowered further down to 14.75 at 1.83 K. The magnetization at 2 K saturates rapidly to 13.98 Bohr magnetons. These experimental values are in good agreement with two Gd^{III} $S = 7/2$ spins (values expected to be respectively 15.75 cm^3 K mol^{-1} and 14 μ_B for $g = 2$) only very weakly antiferromagnetically coupled. Such a coupling can only occur within the carboxylate-bridged dimers present in the structure of **3**. Indeed, the temperature dependence of χT is satisfactorily reproduced (full line in Figure 8) by the equation deduced from the isotropic spin Hamiltonian $\boldsymbol{H} = -J(S_{Gd1} \cdot S_{Gd2})$, to which a term to take into account the TIP has been added. This equation[43] is

$$\chi = \frac{2N_A\beta^2g^2}{k_BT} \times \left[\frac{e^x + 5e^{3x} + 14e^{6x} + 30e^{10x} + 55e^{15x} + 91e^{21x} + 140e^{28x}}{1 + 3e^x + 5e^{3x} + 7e^{6x} + 9e^{10x} + 11e^{15x} + 13e^{21x} + 15e^{28x}}\right] + \text{TIP}$$

with $x = J/k_BT$, J being the isotropic interaction parameter. The parameters giving the best agreement with experimental data are thus found to be $J/k_B = -0.028(1)$ K, $g = 2.015(1)$, and TIP = $6.1(3) \times 10^{-4}$ cm^3 K mol^{-1}. The obtained exchange coupling constant compares well with that observed for a similar $Gd_2(\mu\text{-O,O}'\text{-carboxylate})_2(\mu\text{-O-carboxylate})_2$ core.[43] Note that a recent theoretical work gathers a number of experimental versus calculated exchange coupling constants for various kinds of Gd^{III} dimeric complexes.[44] The value found here for compound **3** is in correct agreement.

Conclusion

Five 3-D isostructural metal-organic frameworks using a series of lanthanides with 2-amino-1,4-benzene dicarboxylic acid have been prepared using solvothermal synthesis. The MOFs adopt a cubic $4^{12}\cdot6^3$ topology with dinuclear metal ions as SBU nodes. Photoluminescence spectra were collected for **2**·2DMF and **4**·2DMF, and magnetic susceptibility data (**1**−**5**) found all five complexes to have weak antiferromagnetic behavior. These MOFs are characterized by the presence of amino groups inside their pores that can be postsynthetically functionalized applying a procedure earlier reported.[22] Current studies are dedicated to the modification of these MOFs by introducing functional groups in a postsynthetic manner and investigating their effect on the photoluminescent/magnetic properties of the resulting materials.

Acknowledgment. Support by the Graduate Research School Combination "Catalysis", a joint activity of the graduate research schools NIOK, HRSMC, and PTN and by the COST program Action D35/0011 is thanked. Coordination of some of our research by the FP6 Network of Excellence "Magmanet" (contract number 515767) is also kindly acknowledged. The Advanced Light Source is supported by the Director, Office of Science, Office of Basic Energy Sciences, of the U.S. Department of Energy under Contract No. DE-AC02-05CH11231.

Supporting Information Available: Global CIF for **1**−**5**, XRPD patterns for **1**−**5** (Figures S1−S5), supramolecular interactions in **2**·2DMF (Figure S6), IR spectra for **1**−**5**, and TGA for **1**−**5**. This material is available free of charge via the Internet at http://pubs.acs.org.

IC8017826

(42) Wan, Y. G.; Zhang, L. P.; Jin, L. P.; Gao, S.; Lu, S. Z. *Inorg. Chem.* **2003**, *42*, 4985–4994.

(43) Panagiotopoulos, A.; Zafiropoulos, T. F.; Perlepes, S. P.; Bakalbassis, E.; Massonramade, I.; Kahn, O.; Terzis, A.; Raptopoulou, C. P. *Inorg. Chem.* **1995**, *34*, 4918–4920.

(44) Roy, L. E.; Hughbanks, T. *J. Am. Chem. Soc.* **2006**, *128*, 568–575.